Biochemical and Biophysical Research Communications 434 (2013) 867–872

Contents lists available at SciVerse ScienceDirect

Biochemical and Biophysical Research Communications

journal homepage: www.elsevier.com/locate/ybbrc

Concentration-dependent oligomerization of cross-linked complexes between ferredoxin and ferredoxin–NADP$^+$ reductase

Yoko Kimata-Ariga *, Hisako Kubota-Kawai, Young-Ho Lee, Norifumi Muraki, Takahisa Ikegami, Genji Kurisu, Toshiharu Hase

Institute for Protein Research, Osaka University, 3-2 Yamadaoka, Suita, Osaka 565-0871, Japan

ARTICLE INFO

Article history:
Received 18 March 2013
Available online 22 April 2013

Keywords:
Ferredoxin
Ferredoxin–NADP$^+$ reductase
X-ray crystal structure
Dynamic light scattering
Cross-linking

ABSTRACT

Ferredoxin–NADP$^+$ reductase (FNR) forms a 1:1 complex with ferredoxin (Fd), and catalyzes the electron transfer between Fd and NADP$^+$. In our previous study, we prepared a series of site-specifically cross-linked complexes of Fd and FNR, which showed diverse electron transfer properties. Here, we show that X-ray crystal structures of the two different Fd–FNR cross-linked complexes form oligomers by swapping Fd and FNR moieties across the molecules; one complex is a dimer from, and the other is a successive multimeric form. In order to verify whether these oligomeric structures are formed only in crystal, we investigated the possibility of the oligomerization of these complexes in solution. The mean values of the particle size of these cross-linked complexes were shown to increase with the rise of protein concentration at sub-milimolar order, whereas the size of dissociable wild-type Fd:FNR complex was unchanged as analyzed by dynamic light scattering measurement. The oligomerization products were detected by SDS–PAGE after chemical cross-linking of these complexes at the sub-milimolar concentrations. The extent and concentration-dependent profile of the oligomerizaion were differentiated between the two cross-linked complexes. These results show that these Fd–FNR cross-linked complexes exhibit concentration-dependent oligomerization, possibly through swapping of Fd and FNR moieties also in solution. These findings lead to the possibility that some native multi-domain proteins may present similar phenomenon *in vivo*.

1. Introduction

Evidences have been shown that some proteins coexist in more than one oligomeric state under physiological conditions, and the ratio of these alternate oligomers can be varied depending on the protein composition or environment [1–4]. One of the common mechanisms for protein oligomerization is domain swapping, which works by converting an intramolecular interface in the monomer to an intermolecular interface between subunits in the oligomer [4]. More than 100 domain-swapped structures have been characterized [5], but the functional and physiological relevance as well as the mechanism of the swapping is often not understood. However, growing evidence supports the hypothesis that domain swapping has diverse biological functions in oligomerization [6–11]; some potential advantages include higher local concentrations of active sites, larger binding surfaces, new active sites at subunit interfaces, the possibility of allosteric control, and economic ways to produce large protein interaction networks and molecular machineries [8,12].

Ferredoxin (Fd) and Fd–NADP$^+$ reductase (FNR) are redox partners responsible for the conversion between NADP$^+$ and NADPH in the plastids of photosynthetic organisms [13,14]. FNR forms a 1:1 complex with Fd, however, in some proteins of the FNR-family such as phthalate dioxygenase reductase [15] and benzoate dioxygenase reductase [16], Fd-like modules are found in domains fused to the N- or C-terminus of the FNR modules. In our previous study, we prepared a series of cross-linked complexes of maize leaf Fd and FNR by introducing, in each case, a specific disulfide bond between the two proteins, so that the two protein moieties assume various configurations [17]. These Fd–FNR cross-linked complexes showed diverse properties of electron transfer between Fd and FNR. In this study, we solved X-ray crystal structures (Fig. 1) of the two different cross-linked complexes which possessed different unique disulfide bonding sites and distinct electron transfer activity. Unexpectedly, both cross-linked complexes formed oligomers by swapping Fd and FNR moieties across the molecules in crystal. In order to verify whether these oligomeric structures are

* Corresponding author. Fax: +81 6 6879 8613.
E-mail address: a-yoko@protein.osaka-u.ac.jp (Y. Kimata-Ariga).

0006-291X/$ - see front matter © 2013 Elsevier Inc. All rights reserved.
http://dx.doi.org/10.1016/j.bbrc.2013.04.033

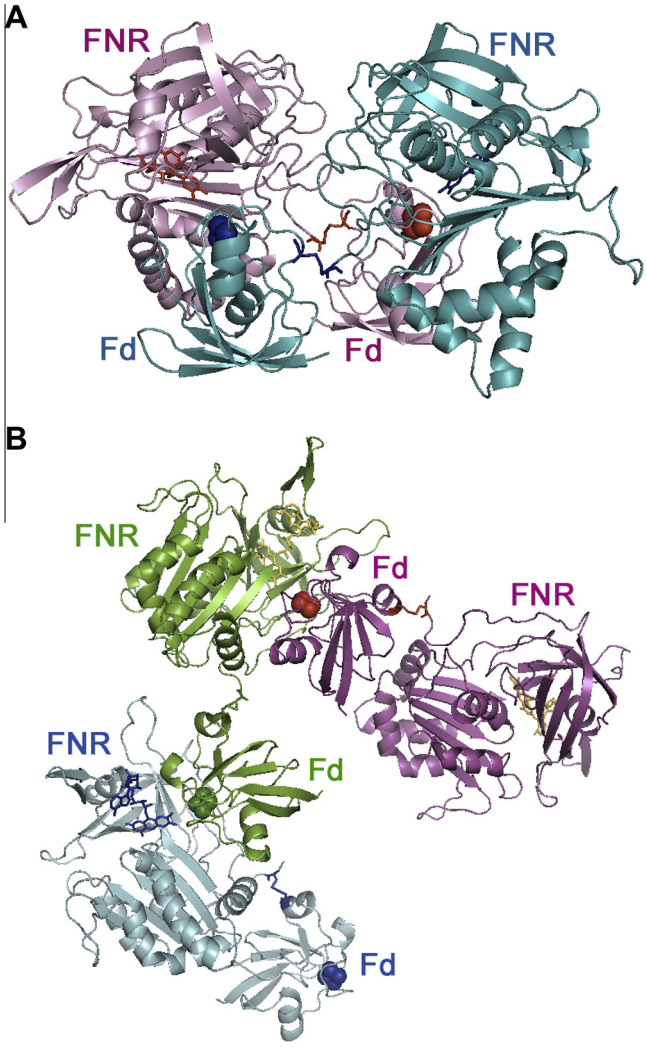

Fig. 1. Ribbon diagram of the crystal structures of Fd4C-FNR1C (A) and Fd5C-FNR1C (B). Individual Fd–FNR molecules are depicted in different colors. The [2Fe-2S] clusters of Fd are shown as spheres. FAD of FNR, and specific cross-linking sites between Fd and FNR are shown with a stick model. Only three Fd5C-FNR1C molecules among successive multimeric structures are depicted in panel B.

formed only in crystal or not, we addressed the possibility of the oligomerization of these cross-linked complexes in solution.

2. Materials and methods

2.1. Preparation of Fd–FNR samples

Preparation of the site-specifically cross-linked complexes, Fd4C-FNR1C and Fd5C-FNR1C, was described previously [17]. Briefly, Fd4C-FNR1C and Fd5C-FNR1C were produced by incubation of each cysteine mutants of FNR (E19C) and Fd (S59C and A70C, respectively) to introduce a unique disulfide-bond between Fd and FNR. Electron transfer activity from FNR- to Fd domain of Fd4C-FNR1C was comparable to that of wild-type FNR with saturating concentration of Fd (at 40 μM), while the activity of Fd5C-FNR1C was reduced by half, as expected from the deduced geometry of Fd and FNR [17].

2.2. Crystallization of the cross-linked Fd–FNR complexes

Fd4C-FNR1C and Fd5C-FNR1C at 0.7 mM and 1.0 mM, respectively were used for crystallization by the hanging drop vapor diffusion method. Equal volume of protein solution (1 μL) and reservoir solution are mixed, and as an additive reagent, 0.5 μL of 5% w/v Octyl-β-D-glucopyranoside and 1 μL of 30% w/v Trimethylamine N-oxide dihydrate were added for Fd4C-FNR1C and Fd5C-FNR1C, respectively. Crystals of Fd4C-FNR1C appeared at 20 °C with 20% PEG6K in 50 mM Tris–HCl pH 7.5 as the reservoir solution. Crystals of Fd5C-FNR1C were obtained at 4 °C with 8% PEG8K and 20% ethylene glycol in 100 mM Bis–Tris pH 6.0 as the reservoir solution. Before freezing the crystals for X-ray data collection, a droplet of Fd4C-FNR1C crystals was incubated in 50% PEG 6K, 50 mM Tris–HCl pH 7.5 and 1% Octyl-β-D-glucopyranoside for 12 h to increase the PEG concentration. Fd5C-FNR1C crystal was directly picked up and freezed by liquid nitrogen.

2.3. X-ray crystallographic studies of the Fd–FNR complexes

All diffraction data were collected at 100 K on the BL44XU beamline at the SPring-8 synchrotron facility (Harima, Japan). Diffraction images were collected using an MX225HE CCD detector (Rayonix, USA) equipped with a Helix Technology cryo-system (Cryo Industries of America, USA), integrated on the CCD camera, and scaled with the HKL-2000 program package [18]. The data collection statistics are summarized in Table 1. The structure of Fd4C-FNR1C was determined by molecular replacement with the program PHASER [19] in the CCP4 program package [20], using Maize Fd1 (PDB ID:3B2F) and FNR1 (PDB ID:1GAW) as the search models. Two Fd–FNR complexes in the crystallographic asymmetric unit were refined at 2.7-Å resolution with the programs coot [21] and REFMAC5 [22] (R_{work}/R_{free} of 22.6/28.0%). Cross-linked disulfide bonds between Cys19 in FNR and Cys59 in Fd were clearly visible in the electron density map, showing the complex as the dimeric form in the swapped manners (Fig. S1A). For Fd5C-FNR1C, the structure was also determined by molecular replacement with the program PHASER. Although the resolution of Fd5C-FNR1C crystal is not good enough to refine the individual temperature factors, crystallographic refinement with tight non-crystallographic

Table 1
Data collection and refinement statistics.

	Fd4C-FNR1C	Fd5C-FNR1C
Wavelength (Å)	0.9	0.9
Resolution range (Å)	150.0–2.68 (2.73–2.68)	50.0–3.80 (3.87–3.80)
Space group	$P2_1$	$P2_1$
Cell dimensions		
a (Å)	59.20	75.17
b (Å)	153.63	120.35
c (Å)	100.12	84.58
β (°)	99.42	109.70
# of Unique reflections	48,206	13,803
R_{merge} (%)	8.7 (20.4)	7.1 (93.9)
Completeness (%)	99.1 (99.0)	98.9 (99.1)
Redundancy	3.6 (3.7)	3.8 (3.8)
Mean I/σ	28.6 (13.0)	25.3 (1.8)
Resolution range (Å)	45.46–2.70	35.67–3.81
Reflections used in refinement	47,570	13,076
R_{total}	0.22902	0.27895
R_{work}	0.22631	0.27745
R_{free}	0.27975	0.30613
No. of refined atoms	12,485	6290
Protein	12,224	6176
Waters	33	0
Other ligands	228	114
R.m.s. deviations		
Bond lengths (Å)	0.0098	0.0100
Bond angles (°)	1.3184	1.3610
Average B-factor (Å^2)	28.921	40.0

restraints was successfully carried out at 3.8-Å with the program REFMAC5 (R_{work}/R_{free} of 27.7/30.6%). Even at the medium resolution, cross-linked sites were observed as the connected electron densities between Fd and FNR (Fig. S1B). In both structures, all amino acid residues except glycine and proline residues are in the stereo-chemically allowed regions in the Ramachandran plot checked with the program MOLPROBITY [23].

2.4. Dynamic light scattering (DLS) measurements

All DLS measurements were performed using a Zetasizer instrument (DynaPro; Wyatt Technology Corporation) at 20 °C with a standard cuvette of 1 cm path length. Protein samples were prepared by diluting the stock solutions (2–3 mM each) of wild-type Fd, FNR, Fd4C-FNR1C and Fd5C-FNR1C dissolved in 50 mM Tris–HCl, pH 7.5 and 100 mMNaCl, with the same buffer, followed by filtrating through MILLEX GV filter (0.22 μm). Measurements were repeated at least three times. Scattering data were collected as an average of 20 scans over 200 s. The data were processed in accordance with the manufacture's software (DYNAMICS; Wyatt Technology Corporation) and presented as scattering intensity of an exponentially decaying autocorrelation. The Stokes–Einstein relationship, together with refractive indices and temperature-corrected viscosities provided by the DYNAMICS software, was used to calculate the hydrodynamic radius of the molecules [24].

2.5. Chemical cross-linking

Fd4C-FNR1C, Fd5C-FNR1C and wild-type Fd:FNR complex, at various concentrations were treated with 5 mM *N*-ethyl-3-(3-dimethylaminopropyl) carbodiimide hydrochloride (EDC) at 25 °C in 25 mM potassium phosphate buffer pH 7.0 and 100 mM NaCl for 1 h. The reaction was terminated by addition of Tris–HCl buffer, pH 7.5 at a final concentration of 0.1 M. For non-reducing SDS–PAGE analysis of the products, SDS–PAGE sample buffer without reducing agents was used. For reducing SDS–PAGE analysis, the reaction mixtures were treated with 20 mM DTT at 25 °C for 10 min, followed by the incubation with SDS–PAGE sample buffer containing 2-mercaptoethanol (0.5% final) at 95 °C for 10 min.

3. Results and discussion

3.1. Differential oligomerization of the two cross-linked complexes of Fd and FNR in crystal

The crystal structures of the site-specifically cross-linked complexes of Fd and FNR, Fd4C-FNR1C and Fd5C-FNR1C, were determined (Fig. 1). To our surprise, both cross-linked complexes exhibit oligomeric structures by swapping their Fd and FNR moieties across the molecules. Moreover, they present different oligomeric structures: Fd4C-FNR1C exhibits a dimer form, and Fd5C-FNR1C is a successive multimeric form. Relative orientation of Fd and FNR moieties intermolecularly interacting in these crystal structures is very similar to that of the complex structure of wild-type Fd:FNR [25] as exemplified in Fig. S2 for Fd4C-FNR1C.

The oligomerization of these cross-linked complexes was originally thought to be an artificial phenomenon which was observed only in the crystal, because electron transfer between Fd- and FNR moieties in the cross-linked complexes was indicated to occur intramolecularly in the previous study [17]. However, the concentration of the cross-linked complexes used in the electron transfer assay was routinely 20 nM, much lower than the physiological concentrations of Fd and FNR which were reported to be 37 μM [26] and >16 μM [27], respectively in the chloroplast stroma, and furthermore, their effective concentrations by considering molecular crowding are thought to be higher than these values. In addition, NMR analysis in the same study [17] using 200 μM of these complexes showed that the almost all signals were considerably broadened, implying significant increases in intermolecular interactions which can be resulted from the oligomerization. Therefore, we investigated the possibility of the oligomerization of the Fd–FNR cross-linked complexes in solution, at various protein concentrations up to the sub-milimolar range.

3.2. Concentration-dependent oligomerization of the Fd–FNR cross-linked complexes in solution

3.2.1. DLS analysis

In order to measure the size of the molecules in solution, DLS analysis was performed using a series of diluent of the protein samples of Fd4C-FNR1C, Fd5C-FNR1C and wild-type Fd:FNR complex. The resulting size distribution histogram as depicted in Fig. S3 shows the peaks defined by the mean value of the hydrodynamic radius of the particle (*R*) and polydispersity, and the *R* values were plotted against protein concentration (Fig. 2). The *R* values of Fd4C-FNR1C and Fd5C-FNR1C at 10 μM were measured to be 3.1 ± 0.1 nm and 2.9 ± 0.1 nm, respectively. These values are similar to those of wild-type Fd:FNR, which are mostly constant (2.9–3.0 nm) throughout the range from 50 to 600 μM (Fig. 2). Thus, Fd4C-FNR1C and Fd5C-FNR1C are thought to be mostly monomer form at 10 μM under the current experimental conditions. However, the mean size of the two cross-linked complexes increased when their samples at higher concentrations were used for the measurement. The size of Fd4C-FNR1C at higher than 300 μM is significantly larger, and gradually increases up to 3.4 ± 0.1 nm at 600 μM. The concentration-dependent increase in the mean size of Fd5C-FNR1C is more pronounced: e.g. 3.4 ± 0.3 nm at 100 μM and 4.0 ± 0.1 nm at 600 μM. The molecular weight of these molecules was estimated by interpolation from the measured particle radius (*R*), based on an empirical curve of known globular proteins [28,29]. The resulting mean values of estimated molecular weight

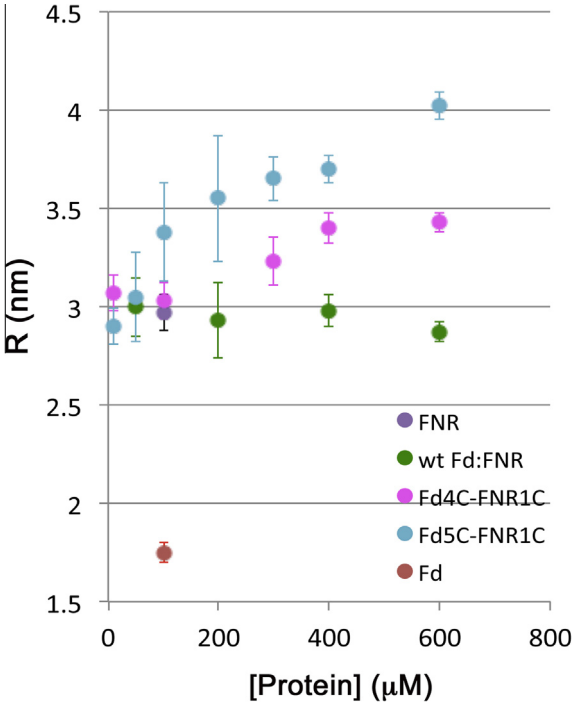

Fig. 2. Particle size of Fd4C-FNR1C, Fd5C-FNR1C and wild-type Fd:FNR complexes. The mean value of the particle size (*R*; radius) at different protein concentrations was obtained by DLS analysis (each 3–5 measurements, exemplified in Fig. S3). The values for free Fd and FNR are also included as references.

at 600 μM are 60 ± 4 kDa for Fd4C-FNR1C and 88 ± 3 kDa for Fd5C-FNR1C, which are 1.3 and 2.1 times larger than those at 10 μM (46 ± 3 kDa and 42 ± 3 kDa, respectively). The latter values are similar to the calculated molecular weight of the cross-linked complexes (45.8 kDa) of maize Fd (10.5 kDa) and FNR (35.3 kDa), consistent with the above description that Fd4C-FNR1C and Fd5C-FNR1C are mostly monomer form at 10 μM.

Furthermore, the size distribution histogram of the cross-linked complexes (Fig. S3) shows that, not only the molecule size (R), but also the peak width representing the polydispersity increases as the concentration of the molecule rises. For example, the % polydispersity (%Pd) for Fd4C-FNR1C and Fd5C-FNR1C is 11 ± 2% and 8 ± 2% at 10 μM, but 16 ± 2% and 17 ± 1% at 600 μM, respectively; the level of homogeneity is generally considered high when the %Pd value is less than 15%. This indicates the increased heterogeneity of the molecule size at the higher concentrations, that is, alternate molecular species such as dimers and/or higher-order oligomers are expected to coexist. In contrast, the polydispersity of the mixture of wild-type Fd and FNR is relatively high (17 ± 4%) at lower concentration (50 μM) but decreases with the increase in concentrations (12 ± 5% at 200 μM and 7 ± 2% at 600 μM). This appears to be consistent with the fact that the proportion of unbound Fd and FNR in the mixture decreases with the rise of the protein concentration; the dissociation constant for the binding between Fd and FNR is several μM.

To sum up, DLS analysis indicates that the oligomerization of the two Fd–FNR complexes leading to the increase in the average particle size occurs in solution as the protein concentration increases to the sub-milimolar order.

3.2.2. Chemical cross-linking analysis

The oligomerization of Fd4C-FNR1C and Fd5C-FNR1C complexes was further addressed by chemical cross-linking analysis. These complexes at different sub-milimolar concentrations were treated with EDC, a bi-functional zero-length cross-linker, and analyzed by non-reducing SDS–PAGE (Fig. 3A). EDC is carboxyl and amine-reactive, and was previously shown to effectively cross-link between spinach Fd and FNR, yielding a 47 kDa product consistent with a 1:1 binding stoichiometry [30]. In agreement with this, treatment of the mixture of wild-type maize Fd and FNR with EDC (Fd:FNR +EDC in Fig. 3A) produced broad, multiple bands with apparent molecular weight of about 40–48 kDa (shown with an arrow), which probably reflect the heterogeneity of cross-linking sites between Fd and FNR. On the other hand, EDC treatment of Fd4C-FNR1C and Fd5C-FNR1C caused significant shifts of the band with widely broad ranges of molecular weight (Fig. 3A). Cross-linking of Fd4C-FNR1C produced broad shifted bands of 75–110 kDa (asterisk in the right side of figure) which slightly increased within the range of 0.2–0.8 mM protein concentration. Increased shifts were observed with Fd5C-FNR1C, and in addition to the main shifted bands of 75–140 kDa, faint bands around 200 kDa were also observed. Thus, significant shifts of the bands at higher molecular weight (>75 kDa) were only observed with the cross-linked complexes, not with dissociable Fd:FNR complex. Therefore,

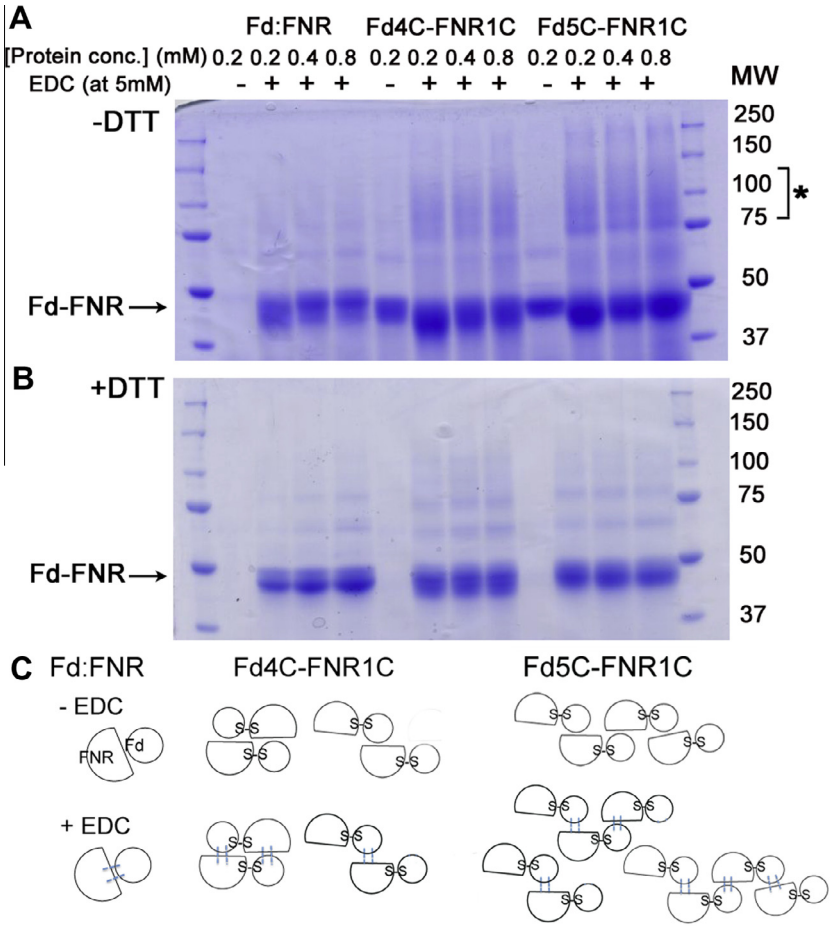

Fig. 3. SDS–PAGE analysis of EDC cross-linked products of Fd4C-FNR1C, Fd5C-FNR1C and wild-type Fd:FNR complexes in the absence (A) and in the presence (B) of DTT. Panel C shows schematic model to explain the results of EDC cross-linking analysis. Dotted lines stand for EDC cross-linking sites which can be up to five in number. So far, it is not clear whether Fd4C-FNR1C forms a closed (left) and/or opened (right) dimer in solution. Refer to Fig. 4S also.

cross-linking experiments also revealed the oligomerization of Fd4C-FNR1C and Fd5C-FNR1C at sub-milimolar concentration in solution. As observed in the DLS analysis, the oligomerization of Fd5C-FNR1C appears to increase compared to Fd4C-FNR1C under the current experimental condition, suggesting the difference in the extent and/or mode of oligomerization depending on the linkage site. The lower level of oligomerization (75–110 kDa) observed with Fd4C-FNR1C suggests that the dimers are formed also in solution at sub-milimolar concentration although whether they are closed or opened form illustrated in Fig. 3C is not clear. On the other hand, in the case of Fd5C-FNR1C, which forms successive multimers in crystal, further oligomerization may take place also in solution. EDC, as a zero-length cross-linker, is expected to connect primarily between the residues located on the productive binding surface of Fd and FNR as illustrated in Fig. 3C (dotted lines); there are five salt-bridges comprising pairs of carboxyl- and amine groups between Fd and FNR. Accordingly, the shift of bands at higher molecular weights, observed in the cases of Fd4C-FNR1C and Fd5C-FNR1C, is estimated to be mainly due to the intermolecular cross-linking between the binding sites of Fd and FNR, caused by the swapping of these molecules (+EDC in Fig. 3C). In a reducing SDS–PAGE (Fig. 3B) after treatment with DTT that cleaves the disulfide bond between Fd- and FNR moieties within Fd4C-FNR1C and Fd5C-FNR1C molecules, the shifted bands at the higher molecular weight largely diminished, which appears to support above estimation. Remaining faint bands at about ~65 kDa and ~82 kDa, also observed in many lanes in Fig. 3, may result from the minor EDC cross-linking within a dimer of FNR which is observed *in vitro* and *in vivo* [31–33], formed by using FNR surface opposite to the Fd-binding surface: ~65 kDa is a possible dimer of FNR, and ~82 kDa is a possible dimer of EDC cross-linked molecule between Fd and FNR.

To conclude, (1) two cross-linked complexes of Fd and FNR formed oligomeric structures by swapping of Fd and FNR moieties across the molecules in crystals, and (2) oligomerization event was also detected in solution depending on their protein concentration. Oligomerization of these two complexes was also suggested by NMR chemical shift perturbation analysis [17]; in our preliminary experiments, significant broadening of signals was observed even at less than 400 μM of Fd5C-FNR1C and at around 400 μM of Fd4C-FNR1C, although for the 1:1 mixture of wild-type Fd and FNR, only slight broadening was observed at more than 1.0 mM. Analytical ultra-centrifugation is another common method to address the size of molecules in solution, but is not suitable for this study because the protein concentration as high as sub-milimolar is beyond the limit to the proper detection of optical density of these proteins. Oligomeric forms of Fd4C-FNR1C and Fd5C-FNR1C were hardly detected by gel filtration and native-PAGE possibly due to the change of the protein concentration during the fractionation.

The changes in the size and oligomerization state at different protein concentrations suggest concentration-dependent conversion between monomers and multimers in solution. Monomer–dimer equilibrium was observed for other domain-swapped proteins [34–37]. For example, ribonuclease A was shown to dimerize at pH 6.5 and 37 °C with the dissociation constant for the dimer of 2.7 mM using enzymatic analysis [34], and response regulator Regx3 exists as both monomers and dimers in a concentration-dependent equilibrium in solution, within the range of 2.7–15.3 mg/ml (corresponding to 0.12–0.7 mM) by SAX measurements; the observed monomer–dimer equilibrium was noted to be fully reversible because the volume fraction of monomers increases by diluting a concentrated sample within a few minutes [35], which was also observed in this study of Fd–FNR cross-linked complexes. The energy balance between monomers and multimers of the two Fd–FNR complexes is not clear, and more extensive thermodynamical analysis such as isothermal titration calorimetry will be needed for this purpose.

In our study, Fd5C-FNR1C was designed to introduce more strain compared to Fd4C-FNR1C when their Fd- and FNR-domains are trying to assume native interaction mode of free Fd and FNR [17]. This could be a reason why Fd5C-FNR1C tends to form multimers whose Fd- and FNR domains are successively exchanged, while oligomer formation is less extensive in Fd4C-FNR1C. The difference in a linker region is also worth describing the control of the swapping process although their energetics is not clear [38–40]. In this connection, so far, no domain swapped structures were obtained for natural Fd–FNR like proteins which possess long, flexible linker region [15,16]. Furthermore, a volume effect such as the molecular crowding effect can be also considered [41,42]; if a domain-swapped multimer assume a more compact conformation than a monomer, oligomerization should be facilitated at higher protein concentrations. A series of systematically designed Fd–FNR cross-linked complexes in our hands should provide rational tool for elucidating the mechanism for differential domain swapping, which would be difficult to achieve just by using collections of various natural proteins.

Findings of concentration-dependent oligomerization of these synthetic Fd–FNR cross-linked complexes may lead to the possibility that some native multi-domain proteins could present similar phenomenon *in vivo*, which could be related to their alternative physiological function.

Acknowledgments

This work was supported by grants-in-aid for Scientific Research on Priority Areas (23570165) from the Japan Society for the Promotion of Science (to Y.K.-A.). Coordinates and structure factors have been deposited in the Protein Data Bank under the following accession numbers: Fd4C-FNR1C, 3W5U; Fd5C-FNR1C, 3W5V.

Appendix A. Supplementary data

Supplementary data associated with this article can be found, in the online version, at http://dx.doi.org/10.1016/j.bbrc.2013.04.033.

References

[1] D.B. Huang, C.F. Ainsworth, F.J. Stevens, M. Schiffer, Three quaternary structures for a single protein, Proc. Natl. Acad. Sci. U. S. A. 93 (1996) 7017–7021.
[2] E.K. Jaffe, Morpheeins – a new structural paradigm for allosteric regulation, Trends Biochem. Sci. 30 (2005) 490–497.
[3] S.H. Lawrence, U.D. Ramirez, L. Tang, et al., Shape shifting leads to small-molecule allosteric drug discovery, Chem. Biol. 15 (2008) 586–596.
[4] A.M. Gronenborn, Protein acrobatics in pairs – dimerization via domain swapping, Curr. Opin. Struct. Biol. 19 (2009) 39–49.
[5] H.M. Berman, J. Westbrook, Z. Feng, et al., The Protein Data Bank, Nucleic Acids Res. 28 (2000) 235.
[6] M.J. Bennett, M.R. Sawaya, D. Eisenberg, Deposition diseases and 3D domain swapping, Structure 14 (2006) 811–824.
[7] S. Hirota, Y. Hattori, S. Nagao, et al., Cytochrome c polymerization by successive domain swapping at the C-terminal helix, Proc. Natl. Acad. Sci. U. S. A. 107 (2010) 12854–12859.
[8] Y. Liu, D. Eisenberg, 3D domain swapping: as domains continue to swap, Protein Sci. 11 (2002) 1285–1299.
[9] M. Czjzek, S. Letoffe, C. Wandersman, et al., The crystal structure of the secreted dimeric form of the hemophore HasA reveals a domain swapping with an exchanged heme ligand, J. Mol. Biol. 365 (2007) 1176–1186.
[10] M. Yamasaki, W. Li, D.J. Johnson, J.A. Huntington, Crystal structure of a stable dimer reveals the molecular basis of serpin polymerization, Nature 455 (2008) 1255–1258.
[11] Z. Wang, T. Matsuo, S. Nagao, S. Hirota, Peroxidase activity enhancement of horse cytochrome c by dimerization, Org. Biomol. Chem. 9 (2011) 4766–4769.
[12] S. Negoro, N. Shibata, Y. Tanaka, et al., Three-dimensional structure of nylon hydrolase and mechanism of nylon-6 hydrolysis, J. Biol. Chem. 287 (2012) 5079–5090.

[13] G.T. Hanke, G. Kurisu, M. Kusunoki, H. Hase, Fd:FNR electron transfer complexes: evolutionary refinement of structural interactions, Photosynth. Res. 81 (2004) 317–327.
[14] N. Carrillo, E.A. Ceccarelli, Open questions in ferredoxin–NADP+ reductase catalytic mechanism, Eur. J. Biochem. 270 (2003) 1900–1915.
[15] C.C. Correll, M.L. Ludwig, C.M. Bruns, P.A. Karplus, Structural prototypes for an extended family of flavoprotein reductases: comparison of phthalate dioxygenase reductase with ferredoxin reductase and ferredoxin, Protein Sci. 2 (1993) 2112–2133.
[16] A. Karlsson, Z.M. Beharry, D.M. Eby, et al., X-ray crystal structure of benzoate 1,2-dioxygenase reductase from Acinetobacter sp. Strain ADP1, J. Mol. Biol. 318 (2002) 261–272.
[17] Y. Kimata-Ariga, Y. Sakakibara, T. Ikegami, T. Hase, Electron Transfer of site-specifically cross-linked complexes between ferredoxin and ferredoxin–NADP+ reductase, Biochemistry 49 (2010) 10013–10023.
[18] Z. Otwinowsk, W. Minor, Processing of X-ray diffraction data collected in oscillation mode, Methods Enzymol. 276 (1997) 307–326.
[19] A.J. McCoy, R.W. Grosse-Kunstleve, P.D. Adams, et al., Phaser crystallographic software, J. Appl. Crystallogr. 1 (40(Pt 4)) (2007) 658–674.
[20] Collaborative Computational Project No. 4. The CCP4 suite: programs for protein crystallography. Acta Crystallogr. D50 (1994) 760–763.
[21] P. Emsley, K. Cowtan, Coot: model-building tools for molecular graphics, Acta Crystallogr. D Biol. Crystallogr. 60 (2004) 2126–2132.
[22] G.N. Murshudov, A.A. Vagin, E.J. Dodson, Refinement of macromolecular structures by the maximum-likelihood method, Acta Crystallogr. D53 (1997) 240–255.
[23] S.C. Lovell, I.W. Davis, W.B. Arendall 3rd, et al., Structure validation by Calpha geometry: phi, psi and Cbeta deviation, Proteins 15 (50(3)) (2003) 437–450.
[24] Z. Adamczyk, B. Cichocki, M.L. Ekiel-Jeżewska, et al., Fibrinogen conformations and charge in electrolyte solutions derived from DLS and dynamic viscosity measurements, Colloid Interface Sci. 385 (2012) 244–257.
[25] G. Kurisu, M. Kusunoki, E. Katoh, T. Yamazaki, K. Teshima, Y. Onda, Y. Kimata-Ariga, H. Hase, Structure of the electron transfer complex between ferredoxin and ferredoxin–NADP+ reductase, Nat. Struct. Biol. 8 (2001) 117–121.
[26] K. Yonekura-Sakakibara, Y. Onda, T. Ashikari, et al., Analysis of the reductant supply systems for ferredoxin-independent sulfite reductase in photosynthetic and nonphotosynthetic organs in maize, Plant Physiol. 122 (2000) 887–894.
[27] S. Okutani, G.T. Hanke, Y. Satomi, et al., Three maize leaf ferredoxin:NADPH oxidoreductases vary in subchloroplast location, expression, and interaction with ferredoxin, Plant Physiol. 139 (2005) 1451–1459.
[28] C. Leyrat, R. Schneider, E.A. Ribeiro Jr., Ensemble structure of the modular and flexible full-length vesicular stomatitis virus phosphoprotein, J. Mol. Biol. 423 (2012) 182–197.
[29] V.N. Uversky, Use of fast protein size-exclusion liquid chromatography to study the unfolding of proteins which denature through the molten globule, Biochemistry 32 (1993) 13288–13298.
[30] G. Zanetti, A. Aliverti, B. Curti, A cross-linked complex between ferredoxin and ferredoxin–NADP+ reductase, J. Biol. Chem. 259 (1984) 6153–6157.
[31] F. Alte, A. Stengel, J.O. Benz, et al., Ferredoxin:NADPH oxidoreductase is recruited to thylakoids by binding to a polyproline type II helix in a pH-dependent manner, Proc. Natl. Acad. Sci. U. S. A. 107 (2010) 19260–19265.
[32] M. Lintala, Y. Allahverdiyeva, H. Kidron, et al., Structural and functional characterization of ferredoxin–NADP+-oxidoreductase using knock-out mutants of Arabidopsis, Plant J. 49 (2007) 1041–1052.
[33] M. Twachtmann, B. Altmann, N. Muraki, et al., N-terminal structure of maize ferredoxin:NADP+ reductase determines recruitment into different thylakoid membrane complexes, Plant Cell 24 (2012) 2979–2991.
[34] C. Park, R.T. Raines, Dimer formation by a "monomeric" protein, Protein Sci. 9 (2000) 2026–2033.
[35] J. King-Scott, E. Nowak, E. Mylonas, et al., The structure of a full-length response regulator from *Mycobacterium tuberculosis* in a stabilized three-dimensional domain-swapped, activated state, J. Biol. Chem. 282 (2007) 37717–37729.
[36] J. Carey, S. Lindman, M. Buuer, S. Linse, Protein reconstitution and three-dimensional domain swapping: benefits and constraints of covalency, Protein Sci. 16 (2007) 2317–2333.
[37] M. Håkansson, A. Svesson, J. Fast, S. Linse, An extended hydrophobic core induces EF-hand swapping, Protein Sci. 10 (2001) 927–933.
[38] F. Rousseau, J.W. Schymkowitz, H.R. Wilkinson, L.S. Itzhaki, Three-dimensional domain swapping in p13suc1 occurs in the unfolded state and is controlled by conserved proline residues, Proc. Natl. Acad. Sci. U. S. A. 98 (2001) 5596–5601.
[39] Y.W. Chen, K. Stott, M.F. Perutz, Crystal structure of a dimeric chymotrypsin inhibitor 2 mutant containing an inserted glutamine repeat, Proc. Natl. Acad. Sci. U. S. A. 96 (1999) 1257–1261.
[40] N.L. Ogihara, G. Ghirlanda, J.W. Bryson, et al., Design of three-dimensional domain-swapped dimers and fibrous oligomers, Proc. Natl. Acad. Sci. U. S. A. 98 (2001) 1404–1409.
[41] R.J. Ellis, Macromolecular crowding: obvious but underappreciated, Trends Biochem. Sci. 26 (2001) 597–604.
[42] H.X. Zhou, G. Rivas, A.P. Minton, Macromolecular crowding and confinement: biochemical, biophysical, and potential physiological consequences, Annu. Rev. Biophys. 37 (2008) 375–397.